의학석사 학위논문

The aggresome has a gel-like structure formed via liquid-liquid phase separation

액체−액체 상 분리를 통해 형성된 젤과 같은 구조를 갖는 응집소체

2022 년 8 월

서울대학교 대학원

의과학과 의과학 전공

박 서 형

액체-액체 상 분리를 통해 형성된 젤과 같은 구조를 갖는 응집소체

지도 교수 이 민 재

이 논문을 의학석사 학위논문으로 제출함

2022년 4월

서울대학교 대학원

의과학과 의과학전공

박 서 형

박서형의 의학석사 학위논문을 인준함

2022년 7월

위 원 장 권 용 태 (인)

부위원장 이 민 재 (인)

위 원 염 진 기 (인)

The aggresome has a gel-like structure formed via liquid-liquid phase separation

Min Jae Lee

Submitting a master's thesis of
Biomedical Sciences

April 2022

Seoul National University
Biomedical Sciences Major

Seo Hyeong Park

Confirming the master's thesis written by
Seo Hyeong Park

July 2022

Chair _____(Seal)
Vice Chair _____(Seal)
Examiner _____(Seal)

Abstract

The aggresome has a gel-like structure formed via liquid-liquid phase separation

Seo Hyeong Park

Major in Biomedical Sciences

Department of Biomedical Sciences

Seoul National University College of Medicine

Liquid-liquid phase separation (LLPS) is a thermodynamic and reversible process in which biological energies go toward the lowest free energy state by demixing a homogeneous liquid phase into two distinct phases. Cytosolic biomolecular condensates such as stress granules and P-bodies are formed by phase separation under cellular stress. When proteasome activity is inhibited, excess amounts of polyubiquitin conjugates are sequestered into juxta-nuclear aggresomes. The aggresome functions as a regulatory point for the global proteostasis, connected with autophagy. Here, I show that the aggresome is assembled through phase separation, but has more gel- or glass-like features than liquid-like characteristics. When I performed fluorescence recovery after photobleaching (FRAP) assays, the

aggresome showed slower and less efficient fluorescence recovery than other reported liquid droplets. Furthermore, treatment with 1,6-hexanediol, which rapidly disrupts other LLPS-mediated protein condensates, resulted in delayed effects on aggresome dissolution. These results suggest that the aggresome is a unique membrane-less organelle with hydrogel-like characteristics. Inhibition of this process resulted in less soluble and more toxic cytoplasmic speckles. Thus, the aggresome is a triage point sequestering cytotoxic aggregation-prone proteins.

* The study is further being explored for publication.

Keywords: proteasome, aggresome, membrane-less organelle, liquid-liquid phase separation

Student number: 2020-22378

Contents

List of figures

List of abbreviations

AD : Alzheimer’s disease

ALS : Autophagy-lysosomal system

ATP : Adenosine triphosphate

BSA : Bovine serum albumin

DMEM : Dulbecco's modified eagle medium

DMSO : Dimethyl sulfoxide

FBS : Fetal bovine serum

FRAP : Fluorescence recovery after photobleaching

FTD : Frontotemporal dementia

IB : Immunoblotting

LLPS : Liquid-liquid phase separation

PB1 : Phox and Bem1

PBS : Phosphate-buffered saline

PQC : Protein quality control

PVDF : Polyvinylidene fluoride

ROI : Region of interest

SDS : Sodium dodecyl sulfate

SDS-PAGE : Sodium dodecyl sulfate-polyacrylamide gel electrophoresis

sfGFP: Superfolder green fluorescent protein

SQSTM1 : Sequestosome 1

TBST : Tris-buffered saline with tween 20

Ub : Ubiquitin

UBA : Ubiquitin-associated

UPS : Ubiquitin-proteasome system

WCEs : Whole-cell extracts

Introduction

Liquid-liquid phase separation (LLPS) is emerging as an essential phenomenon in various fundamental cellular processes, including signal transduction, gene expression, and biochemical reactions by creating distinct physical and biochemical compartments [1, 2]. LLPS leads to a de-mixing of a homogeneous liquid phase into two distinct phases, a dilute phase and a dense phase that is referred to as a membrane-less organelle [3]. In eukaryotic cells, several membrane-less organelles, such as stress granules, P-bodies, nucleoli, and heterochromatin, display characteristics of liquid-like structures [4-6]. Such compartmentalization provides benefits to cells, allowing biomolecules to be concentrated within the compartment while continuously exchanging with the surrounding environments [1, 7].

Phase-separated liquid-like structures can transition into more stable states, such as a gel-like state which show reduced mobility, or an inert solid state [8-10]. Phase transition is modulated by diverse factors that affect multivalent interactions, including the concentration of components, composition, chaperones, and other environmental factors such as pH, temperature, and salt concentration [4, 11]. It is also known that liquid-like structures can solidify into harmful aggregates of amyloids in response to stress or mutations which can result in the gradual development of neurodegenerative diseases, such as frontotemporal dementia (FTD), amyotrophic lateral sclerosis (ALS), and Alzheimer's disease (AD) [12, 13].

Maintaining the protein homeostasis, proteostasis, is crucial for cell viability [14]. Cells have developed protein quality control (PQC) mechanisms that strictly maintain and

control the balance between protein synthesis, folding, and degradation [15]. The constant regulation of proteins by chaperones and the action of two protein degradation systems, the ubiquitin-proteasome system (UPS) and the autophagy-lysosome system (ALS), are crucial to these quality control [16-19]. Molecular chaperones facilitate the protein folding and refolding of misfolded proteins. If misfolded proteins fail to refold, molecular chaperones can also mediate their degradation in collaboration with cellular proteolytic pathways. However, misfolded proteins that survive the attempts of molecular chaperones to refold or degrade eventually result in protein dysfunction and cytotoxic protein aggregates.

When the cellular capacity of degradation machinery is exceeded, misfolded protein aggregates and to-be-degraded proteins spontaneously accumulate into the inclusion body [20-22]. Under the condition, misfolded or polyubiquitinated proteins are actively segregated into a perinuclear structure, the aggresome, via dynein-mediated retrograde transport to the microtubule-organizing center (MTOC) [23, 24]. In addition to the proteolysis substrates, components of the UPS, molecular chaperones, and the autophagic machinery are co-segregated to the aggresome [20, 25-27]. The autophagosome cargo protein SQSTM1/p62 has also been implicated in aggresome formation by contributing to the transport of both ubiquitinated and non-ubiquitinated proteins [28-30]. Aggresome formation is generally regarded to be a cytoprotective response for segregating proteins from the cytoplasmic environment. Furthermore, the previous study has presented the aggresome serves as a triage point for proteasome recovery and autophagic degradation [31]. The aggresome has an exceptionally large size (~5 μm) and is a dynamic, reversible structure formed under stress conditions, but the characteristics of the aggresome as a liquid droplet-like condensate are still poorly

understood.

Here, I show that the aggresome is a gel-like state that is mediated by LLPS. Furthermore, inhibition of aggresome formation caused cytoplasmic speckles that were more cytotoxic and less mobile than the aggresome. These results will provide insights into the aggresome dynamic as an efficient proteolytic response to stress.

Material and Methods

Mammalian cell culture

Mammalian cells used in this study, including HeLa tetracycline-on (Tet-on) cells expressing sfGFP-Ubiquitin (HeLa-sfGFP-Ub), and HeLa cells stably expressing GFP-p62 and mCherry-Ubiquitin (HeLa-sfGFP-p62 & mCherry-Ub cells) [32] were cultured in Dulbecco's modified Eagle's medium (DMEM), and A549 cells were maintained in Roswell Park Memorial Institute 1640 medium (RPMI-1640) supplemented with 10% (v/v) FBS, 2 mM L-glutamine, and 100 unit/mL penicillin/streptomycin. Cells were sustained in a humidified incubator with 5% CO_2 at 37°C. For various experiments, biochemical reagents were as follows: MG132 (M-1157, AG Scientific), doxycycline (446060050, Acros Organics), nocodazole (M1404, Sigma), sodium arsenite (S7400, Sigma), and 1,6-hexanediol (240117, Sigma).

Immunofluorescence microscopy

Cultured cells on a cover glass were fixed with 4% paraformaldehyde at room temperature for 20 min and then permeabilized with 0.5% Triton X-100 in PBS for 15 min. Before antibody incubation, cells were blocked with 2% BSA in PBS for 30 min. The cells were incubated with primary antibodies in the blocking solution for 2 h. Next, the cells were incubated with Alexa Fluor 488 or 594-conjugated secondary antibodies for 40 min and then mounted with a 4′,6-diamidino-2-phenylindole (DAPI)-containing mounting solution (ab104139, Abcam). Most of the fluorescent signals were monitored and captured using a Revolve Fluorescence microscope by Echo or Olympus fluorescence microscope (IX71).

Images were processed using Adobe Photoshop CC. Within each figure, all images were captured using identical microscope settings and representative of the whole cell population. The primary antibodies used in this study were as follows: anti-SQSTM1 (ab56416, 1:100, Abcam), anti-PSMB5 (PA1977, 1:100, Pierce), anti-G3BP1 (ab56574, 1:300, Abcam). The following secondary antibodies were purchased from Abcam: Alexa Fluor 488-conjugated anti-rabbit (ab150077, 1:1000), Alexa Fluor 594-conjugated anti-mouse (ab150108, 1:1000).

Analysis of soluble and insoluble fraction

For analysis of soluble and insoluble fractions, cultured cells were washed with PBS and lysed with RIPA buffer (50 mM Tris-HCl [pH 8.0], 1% of NP-40, 0.5% of deoxycholate, 0.1% of sodium dodecyl sulfate (SDS), and 150 mM NaCl), all supplemented with protease inhibitors. The lysates were then centrifuged at 16,000 × g for 15 min at 4 ℃. The supernatants were designated as a detergent-soluble fraction. The pellets were washed with lysis buffer and then centrifuged at 16,000 × g for 15 min at 4 ℃. The pellets were resuspended with SDS sample buffer (12.6% glycerol, 160 mM Tris-HCl [pH 6.8], 0.01% (w/v) bromophenol blue, 20 mg/mL SDS, and 5% β-mercaptoethanol), boiled at 100 ℃ for 15 min, and analyzed as a detergent-insoluble fraction. A detergent-soluble fraction was boiled at 80 °C for 10 min in SDS sample buffer, and detergent-soluble, insoluble fractions were analyzed by immunoblotting.

Immunoblotting

For immunoblotting, proteins were separated by SDS-PAGE and then transferred to polyvinylidene difluoride (PVDF) membranes. The membranes were blocked with 5%

skim milk in TBST (25 mM Tris-HCl [pH 7.5], 137 mM NaCl, 2.7 mM KCl, and 0.05% (v/v) Tween 20), and incubated with primary antibodies at 4 °C overnight. The primary antibodies and dilution factors used in this study were as follows: anti-ubiquitin (sc-8107, 1:3000, Santa Cruz Biotechnology), anti-SQSTM1 (ab56416, 1:5000, Abcam), anti-GFP (sc-9996, 1:1000, Santa Cruz Biotechnology), anti-PSMC2 (sc-166972, 1:3000, Santa Cruz Biotechnology), anti-PSMA4 (BML-PW8115, 1:3000, Enzo Life Science), and β-actin (A1978, 1:5000, Sigma). After then, the membranes were washed with TBST and followed by Secondary antibodies (horseradish peroxidase-conjugated anti-mouse IgG [31430, 1:10000, Thermo Fisher] and anti-rabbit IgG [31460, 1:10000, Thermo Fisher] antibodies).

Assessment of cell viability

This property was assessed by the CellTiter-Glo Luminescent Cell Viability Assay (Promega) kit following the manufacturer's protocol. Briefly, HeLa-sfGFP-Ub cells were seeded at densities of 10,000 cells/well in 100 μl in black-wall/clear-bottom 96-well plates, treated with either MG132 (5 μM) or nocodazole (1 μM) in the presence of doxycycline (0.1 μg/ml), and then luminescence substrates were added in the same volume as the cell culture medium. The mixture was incubated for 10 min at room temperature on a shaker, followed by luminescence measurements.

FRAP analysis

For FRAP analysis, HeLa-sfGFP-Ub or HeLa-sfGFP-p62 & mCherry-Ub cells were cultured on PDL-coated glass coverslips. FRAP experiments were performed using Nikon A1 confocal microscope (Nikon) with a 60 × oil immersion lens (1.40 N.A.) and Nikon

imaging software (NIS-Elements) to accomplish photobleaching of circular region of interest (ROI) by laser pulse emission. Time-lapse images were acquired every 10 s for 30 s before bleaching ROIs were photobleached with either 488 nm laser (20 %) or 561 nm laser (15 %) for 1 s. Fluorescence recovery was subsequently imaged every 10 s for 10 min. The Fluorescence intensity of the bleached ROIs over time was measured and normalized to the initial values.

1,6-hexanediol treatment

For treatment with 1,6-hexanediol, complete media (DMEM supplemented with 10% FBS, 2 mM l-glutamine and 100 unit/mL penicillin/streptomycin.) was prepared containing 2% (v/v) 1,6-hexanediol with MG132 (5 μM) or sodium arsenite (0.5 mM). Media was exchanged and replaced with 2% 1,6-hexanediol containing media for indicated periods at room temperature.

Results

Inhibition of proteasomes causes the formation of the aggresome

When proteasome is reversibly or irreversibly inhibited, excess polyubiquitinated and misfolded proteins are sequestered into perinuclear aggresome [20]. To investigate the further characterization of the aggresome, I first confirmed the formation of aggresomes in HeLa Tet-on cells expressing sfGFP-Ubiquitin (Ub). After treatment of the cells with 5 μM MG132 for 16 h, the sfGFP-Ub signal was accumulated in the aggresome (Figure 1). When immunostaining with SQSTM1, one of the aggresome markers, endogenous SQSTM1 was co-localized with sfGFP-Ub.

To inhibit aggresome formation, I cotreated the cells with nocodazole, a microtubule-disrupting drug, and MG132. Because aggresome formation is dependent on microtubule-based transport and develops at the microtubule organizing center (MTOC) [33], nocodazole treatment resulted in small speckled puncta throughout the cytoplasm instead of forming the aggresome (Figure 1).

Under the same condition, I conducted an immunoblotting analysis of fractionated whole-cell extracts (WCEs). When the cells were treated with MG132 for 16 h, both proteasome CP and RP subunits were significantly increased in the Triton X-100-insoluble fraction. The amounts of SQSTM1 oligomeric forms and total polyUb-conjugates were also elevated in the insoluble fraction. Cotreatment with nocodazole induced more protein accumulation in the insoluble fraction than treatment with MG132 alone (Figure 2). Furthermore, cotreatment with nocodazole and MG132 resulted in significantly elevated cytotoxicity, whereas MG132 or nocodazole alone did not affect the cell viability (Figure 3).

Collectively, it was confirmed that prolonged proteasome inhibition induces the accumulation of polyubiquitylated proteins, autophagic receptor p62, and the inhibited proteasome into the aggresome. Furthermore, when this process is inhibited, proteins were more densely accumulated than the aggresome, resulting in more toxic and more insoluble aggregates.

Proteins in the aggresome are more mobile than those in cytoplasmic speckles

To examine whether the aggresome is a liquid condensate formed through liquid-liquid phase separation (LLPS), I analyzed the mobility of sfGFP-Ub in the aggresome using fluorescence recovery after photobleaching (FRAP) in comparison with cytoplasmic speckles. In this assay, the laser light irreversibly bleaches the fluorescent signal of molecules in the region of interest (ROI) and photobleached molecules diffuse away from the bleached spot and are replaced with new fluorescent molecules, resulting in a recovery of the fluorescent signal. Therefore, the fluorescence recovery of labeled proteins within the compartment implies rapid reorganization of diffusional exchange, providing information on the mobility or solubility of components.

Aggresomes or cytoplasmic speckles were designated as a ROI and the fluorescence recovery rate was observed following photobleaching the ROI. If the bleached molecules are in the liquid phase, completely mobile, the mobile fraction is expected to be ~100% with rapid recovery of fluorescence [34]. However, the mobile fraction in the aggresome was less than 50% unlike showing high mobility of proteins within the liquid-like condensates (Figure 4). Known liquid reference proteins, such as nucleolar NPM1, showed ~100% of the mobile fraction [35]. This slow and incomplete recovery within the aggresome suggests that the aggresome adopts a specific conformation

that is best described by a gel-like state. However, sfGFP-Ub mobility in the aggresome was much higher compared to cytoplasmic speckles that did not show any redistribution of fluorescent signals (~10% vs. ~40% recovery at 10 min, Figure 4).

The FRAP results are consistent with immunoblot data (Figure 2) that the proteins in cytoplasmic speckles showed more insoluble characteristics than those in the aggresome. Taken together, the aggresome is a gel-like state and less dynamic than liquid-like condensates, but more dynamic than aggregates. Furthermore, these results suggested that the aggresome could play a role in the clearance of misfolded, nonfunctional proteins and allow proteins within the aggresome to return to cytosol when they recover their activities.

Different positions within the aggresome have little difference in mobility

The aggresome is a large protein inclusion with a diameter of ~ 5 μm, which is enlarged by the aggregation of proteins in response to proteotoxic stress [36, 37]. It was assumed that the dynamic exchange of the proteins located outside and inside the aggresome would be different. In order to confirm the protein mobility according to the position within the aggresome, FRAP assays were performed in HeLa-sfGFP-Ub cells. The core part and the border part within the aggresome were designated as a region of interest (ROI), respectively, and the fluorescence recovery rate was observed following photobleaching the ROI. The border part showed slightly faster fluorescence recovery rates compared to the core part, but there was no significant difference between them (Figure 5). The recovery rates in two distinct locations were confirmed to be comparable to the overall recovery pattern for the aggresome observed in the previous FRAP assay results. These results indicated that the aggresome is a homogeneous state and proteins in the aggresome can exchange among the aggresome as well as between the aggresome and the surrounding

cytosol.

Dynamic features between p62 and ubiquitin within the aggresome

The aggresome contains numerous types of proteins, such as ubiquitin, E3 ubiquitin ligases, proteasome subunits, molecular chaperones, and autophagic components [38]. These diverse proteins function to form and maintain aggresome integrity. Especially poly-ubiquitination is usually required for p62-mediated aggresome formation, and several p62 substrates proceed to the aggresome. Ubiquitinated proteins and p62 are located differently within the aggresome, and I previously observed that p62 was located much outward than ubiquitin (figure 1).

To investigate whether p62 and ubiquitin exhibit different biophysical behavior depending on their spatial location inside the aggresome, FRAP assay was performed using the HeLa cell line stably co-expressing sfGFP-p62 and mCherry-ubiquitin. Although the fluorescent signal of sfGFP-p62 recovered slightly faster than that of mCherry-Ub, there was no statistical difference between them (Figure 6). The overall recovery rate of p62 and Ub was ~40%, showing a similar pattern to that of previous data (Figure 4). Although p62 and ubiquitin in the aggresome have distinct functions and spatial organization, the mobility of p62 within the aggresome is comparable to ubiquitin, and both of them showed gel-like features.

The aggresome has less dynamic and gel-like properties than liquid-like condensates

Additionally, to confirm whether LLPS is necessary for aggresome formation, I treated A549 cells with 1,6-hexanediol (1,6-HD). 1,6-HD, aliphatic alcohol, has been widely used

to study the formation process of the membrane-less cytoplasmic/nuclear condensates, generated via LLPS [39, 40] and it inhibits weak hydrophobic protein-protein or protein-RNA interactions required for the formation of liquid droplet-like condensates [40]. The addition of 1,6-HD did not drastically dissipate the aggresome, unlike stress granules which are rapidly disrupted following 1,6-HD treatment (Figure 7, 8). Nevertheless, 1,6-HD treatment slightly decreased the size and the number of aggresomes compared to the controls. These results are consistent with the results of the previously observed FRAP assay, in which the mobile fraction was less than 50%. Collectively, these results implied that the aggresome is a gel-like phase with optimal solubility suitable for reversible sequestration of proteins under cellular stress.

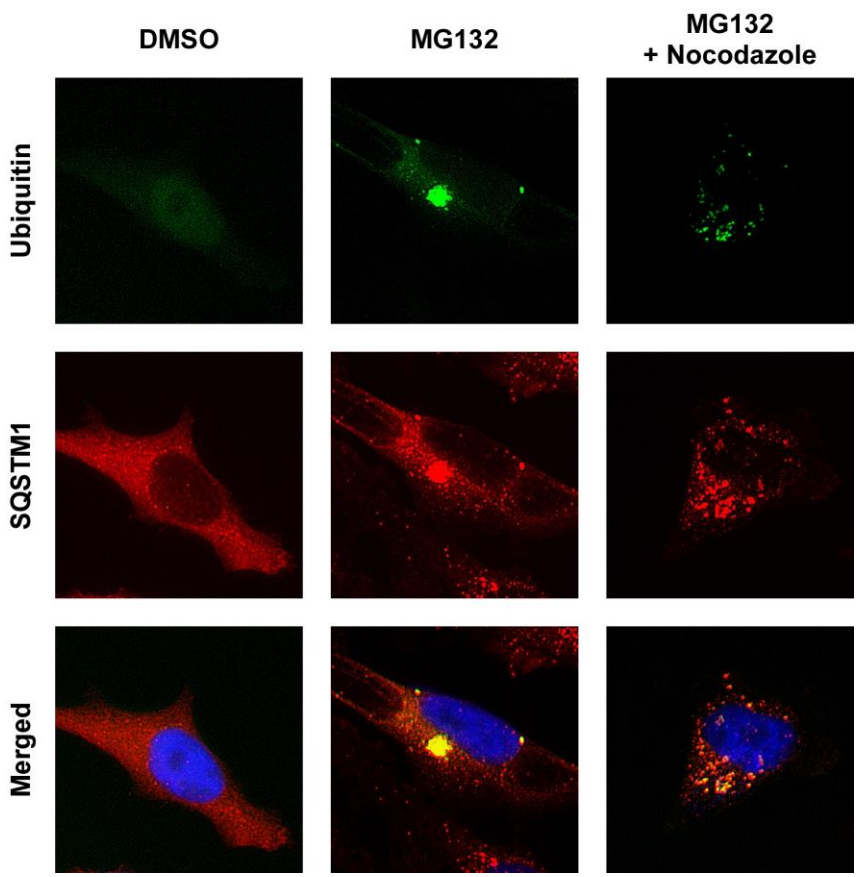

Figure 1. GFP-ubiquitin forms the aggresome upon proteasome inhibition.

Fluorescence microscopy images of immunostaining with anti-SQSTM1 (red) antibody and sfGFP-ubiquitin (green) using HeLa tetracycline-on cells over-expressing sfGFP-Ub in the presence of doxycycline (0. 1 μg/ml) with MG132 (5 μM) or cotreatment of MG132 and nocodazole (1 μM) for 16 h. Nuclei were counterstained with DAPI (blue).

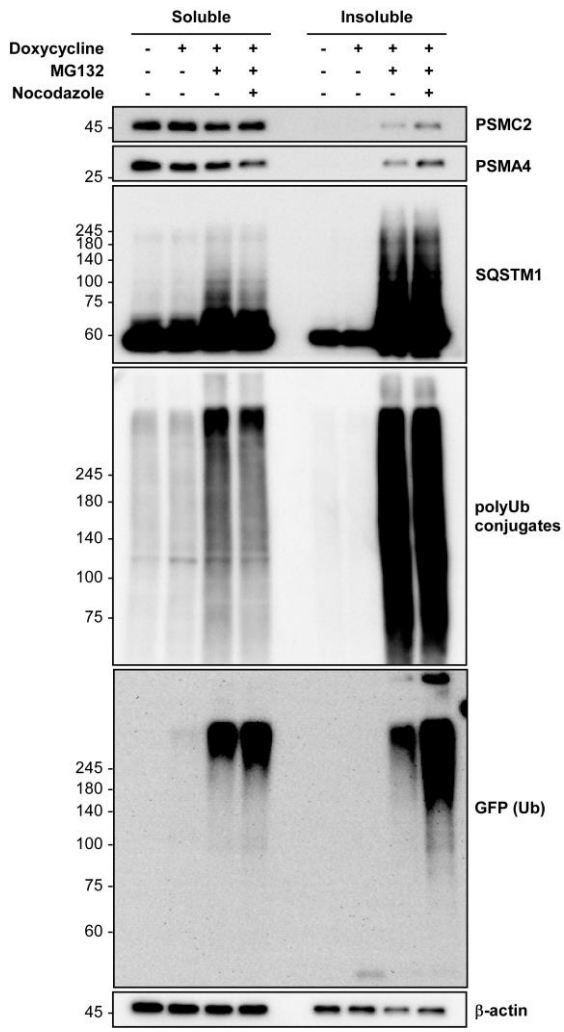

Figure 2. Proteasome inhibitors induce the accumulation of proteins in the insoluble fraction.

HeLa-sfGFP-Ub cells were separated into soluble and insoluble fractions. Cells were treated with MG132(5 μM, 16 h) or cotreatment with MG132(5 μM, 16 h) and nocodazole(1 μM, 16 h) in the presence of doxycycline (0.1 μg/ml, 16 h). Accumulation of SQSTM1, polyubiquitinated proteins, and proteasome subunits in the insoluble fraction was analyzed by SDS-PAGE/immunoblotting (IB) with the indicated antibodies.

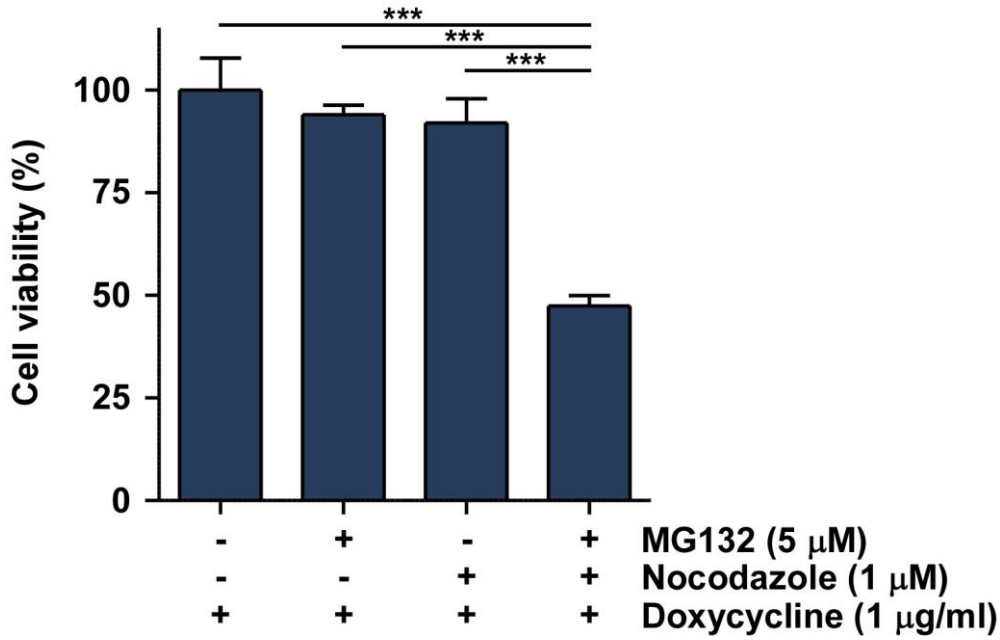

Figure 3. Inhibition of aggresome formation enhances the cytotoxic effects.

Cell viability was measured after 5 μM MG132 treatment in the presence or absence of nocodazole (1 μM) in HeLa-sfGFP-Ub cells. Values are presented as mean ± SD (n = 3); *** $p < 0.001$ (one-way ANOVA with Bonferroni's multiple comparison test).

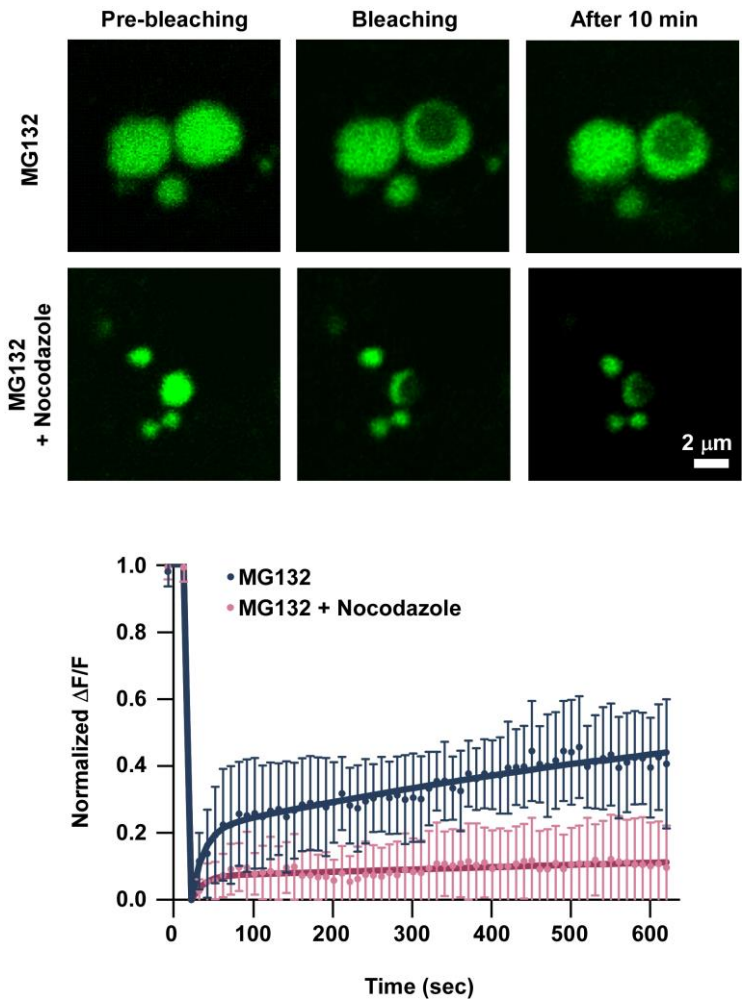

Figure 4. Disparate mobility of misfolded proteins in the aggresome and cytoplasmic speckles.

Fluorescence recovery after photobleaching of the aggresome and cytoplasmic speckles in HeLa-sfGFP-Ub cells. (*top*) The images correspond to the region of interest (ROI) with pre-bleach and post-bleach at t=0 s and t=600 s. (*bottom*) Normalized fluorescence recovery curves indicate that the aggresome appears to recover the fluorescent signals following bleaching, while no recovery was detected for cytoplasmic speckles. Representative results from 12 and 14 independent experiments each. Scale bar: 2 μm.

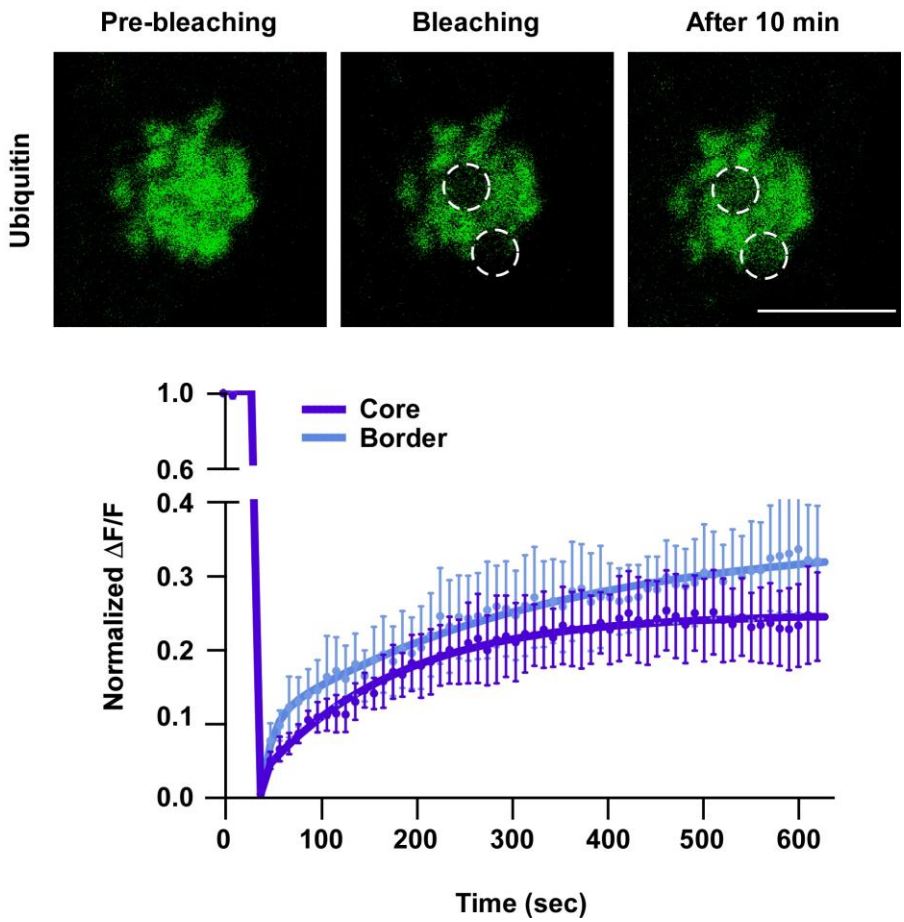

Figure 5. Confirmation of homogeneous state within the aggresome by FRAP assay.

FRAP assay of aggresome at the core and border parts in MG132 (5 μM,16 h)-treated HeLa-sfGFP-Ub cells. (*top*) The images correspond to the region of interest (ROI) with pre-bleach and post-bleach at t=0 s and t=600 s. (*bottom*) Normalized fluorescence recovery curves for different positions within the aggresome. Representative results from 22 independent experiments. Scale bar: 5 μm.

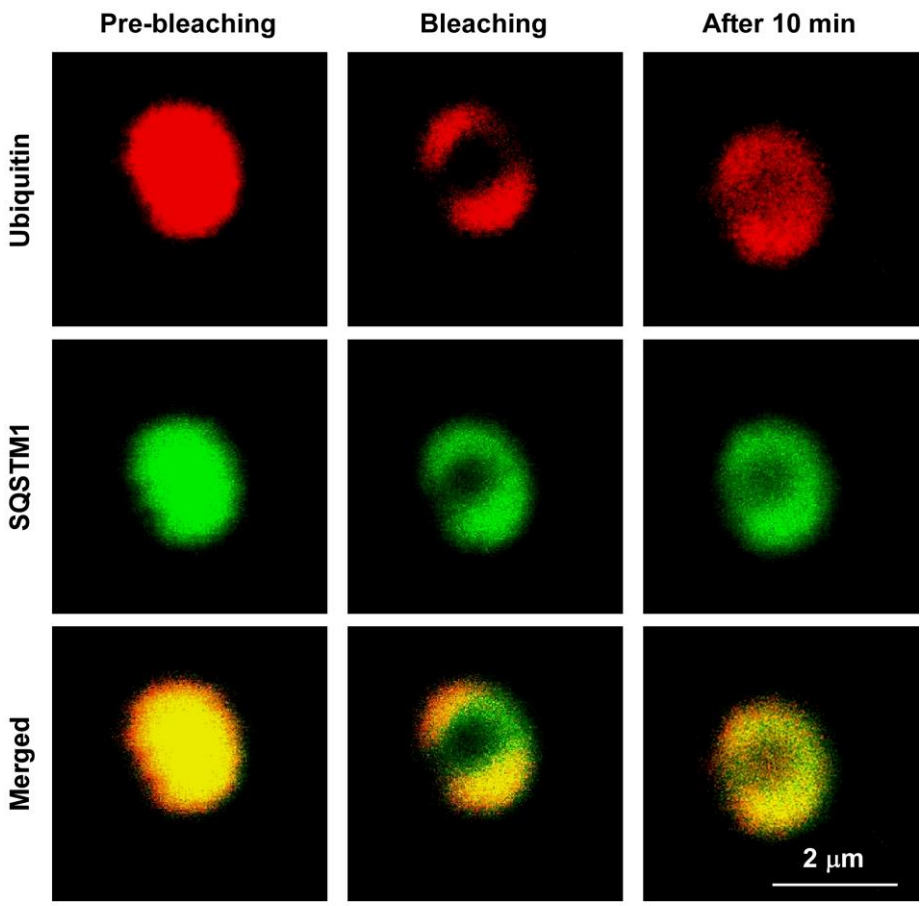
Pre-bleaching
Bleaching
After 10 min
Ubiquitin
SQSTM1
Merged
2 μm

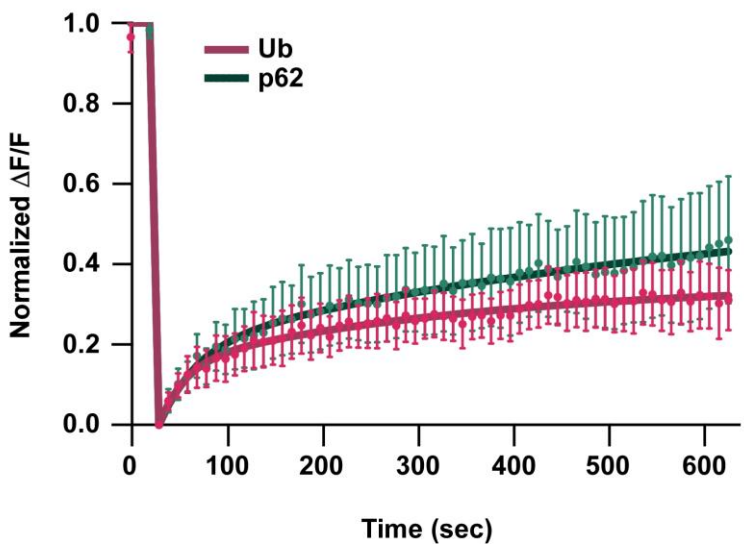
Ub
p62
Normalized ΔF/F
1.0
0.8
0.6
0.4
0.2
0.0
0
100
200
300
400
500
600
Time (sec)

Figure 6. Comparison of dynamic features between ubiquitin and p62.

FRAP assay in MG132 (5 μM,16 h)-treated HeLa-sfGFP-p62 & mCherry-Ub. (*top*) The images correspond to the region of interest (ROI) with pre-bleach and post-bleach at t=0 s and t=600 s. (*bottom*) Normalized fluorescence recovery curves for p62 and Ub within the aggresome. Representative results from 29 independent experiments. Scale bar: 2 μm.

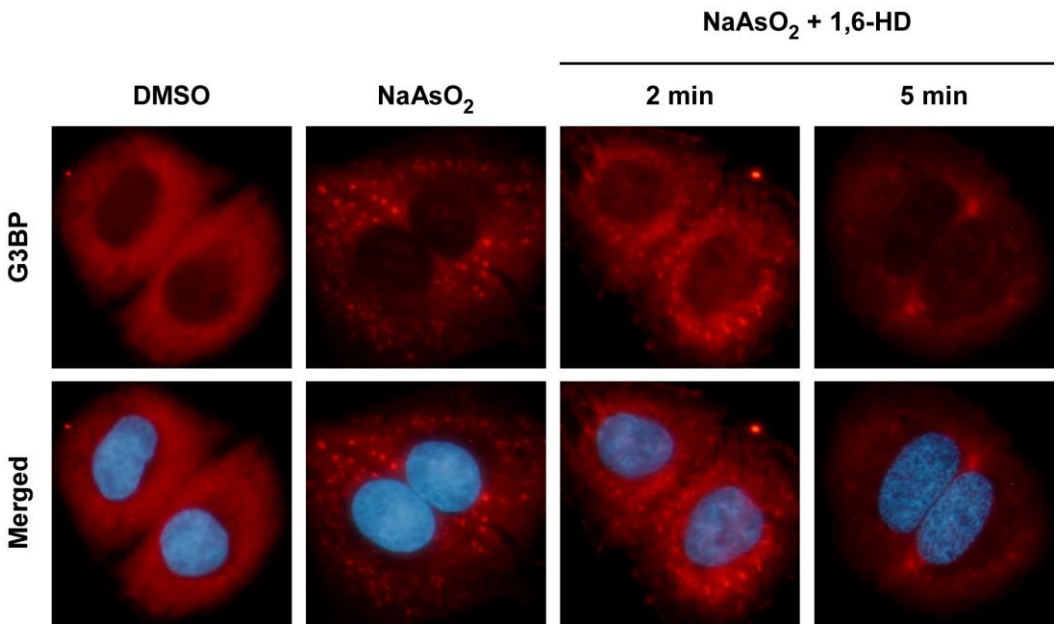
NaAsO2 + 1,6-HD
DMSO
NaAsO2
2 min
5 min
G3BP
Merged

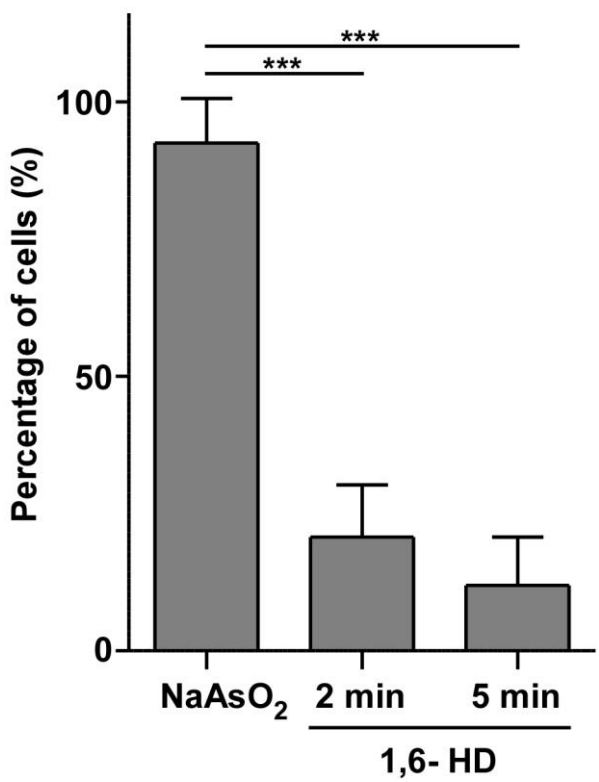
***
***
100
50
0
Percentage of cells (%)
NaAsO2
2 min
5 min
1,6- HD

Figure 7. Treatment of 1,6-hexanediol dissolves stress granules in A549 cells.

Effects of 1,6-hexanediol on $NaAsO_2$-induced stress granules in A549 cells. A549 cells were stressed with $NaAsO_2$ (0.5 mM, 30 min). In the presence of $NaAsO_2$, 2% 1,6-hexanediol was additionally treated for the indicated time. (*top*) Immunostaining with anti-G3BP1 (red) antibody. Nuclei were counterstained with DAPI (blue). (*bottom*) Time-dependent changes in the number of cells that have stress granules after 1,6-hexanediol treatment. n = 114 (NaAsO2), 71 (NaAsO2 +1,6-HD 2 min), 39 (NaAsO2 +1,6-HD 5 min) cells from two independent assays. Values are means ± SD. *** $p < 0.001$ (one-way ANOVA with Bonferroni's multiple comparison test).

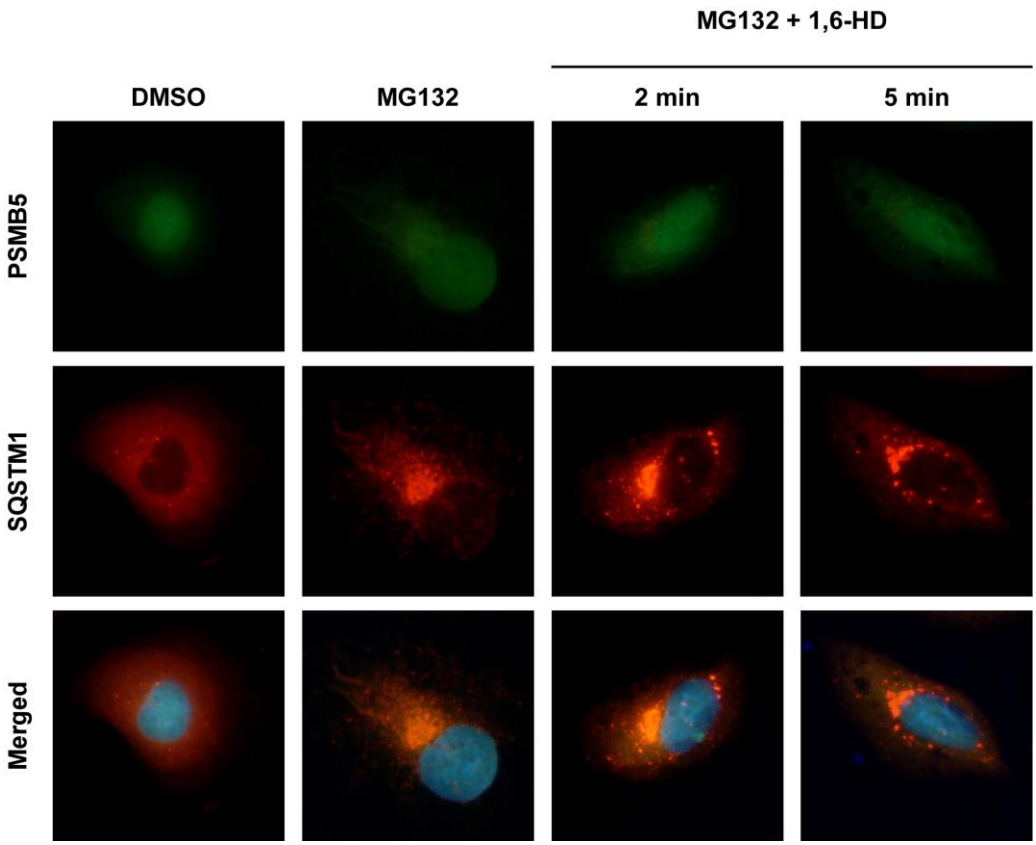
MG132 + 1,6-HD
DMSO
MG132
2 min
5 min
PSMB5
SQSTM1
Merged

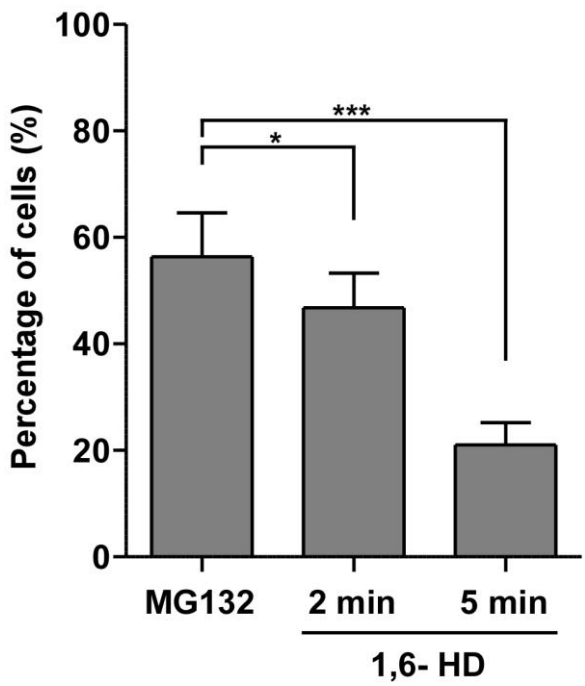
100
80
60
40
20
0
Percentage of cells (%)
***
*
MG132
2 min
5 min
1,6- HD

Figure 8. The aggresome is not rapidly disrupted by 1,6-hexanediol in A549 cells.

Effects of 1,6-hexanediol on MG132-induced the aggresome in A549 cells. A549 cells were treated with MG132 (5 μM, 16 h). In the presence of MG132, 2% 1,6-hexanediol was additionally treated for the indicated time. (*top*) Immunostaining with anti-PSMB5 (green) and SQSTM1 (red) antibodies. Nuclei were counterstained with DAPI (blue). (*bottom*) Time-dependent changes in the number of cells that have aggresomes after 1,6-hexanediol treatment. n = 152 (MG132), 132 (MG132+1,6-HD 2 min), and 139 (MG132+1,6-HD 5 min) cells from two independent assays. Values are means ± SD. * $p < 0.05$, *** $p < 0.001$ (one-way ANOVA with Bonferroni's multiple comparison test).

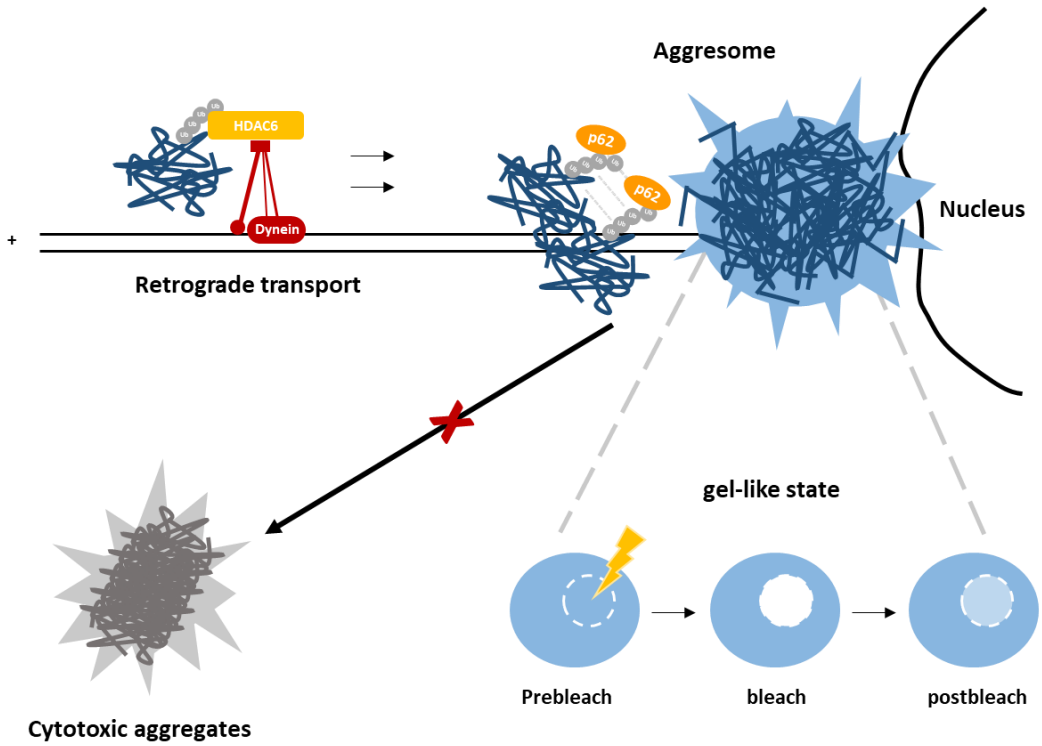

Figure 9. Characteristics of the aggresome as a gel-like condensate.

A proposed model for dynamic characteristics of the aggresome as a unique membrane-less organelle. The aggresome which is generated under intracellular stress is formed through LLPS, and it has gel-like properties. Moreover, inhibition of this process resulted in less soluble and more toxic cytoplasmic speckles. This reversible assembly of the aggresome is expected to be cytoprotective and implicated in solid-like assemblies of amyloidogenic proteins.

Discussion

Here, I report on the dynamic characteristics of the aggresome formed via LLPS under proteotoxic stress. Although several studies have reported on formation and degradation of the aggresome and the proteins that play a role in maintaining integrity of the aggresome and mediating degradation through autophagy, the dynamic properties of the aggresome as a membrane-less structure remain essentially unknown. In my experiments, I confirmed that the aggresome has a gel-like state with low mobility, rather than liquid-like states with high mobility. This suggests that the LLPS acts as a precursor to the formation of aggresome and the aggresome is in an intermediate state during the liquid-solid phase transition. Therefore, my findings collectively indicate that aggresome formation mediates LLPS to reversibly segregate proteins through spatiotemporal sequestration, serving as an efficient cytoprotective mechanism under proteotoxic stress.

In yeast, there are two cytoplasmic quality control compartments, the juxtanuclear quality control (JUNQ) and the insoluble protein deposit (IPOD), responsible for managing misfolded and aggregated proteins. Components of JUNQ show high mobility through the cytosolic compartments, while those of IPOD have less mobility, and amyloidogenic proteins are preferentially directed to IPOD [41]. Two distinct compartments exhibit comparable features to the aggresome and cytoplasmic puncta respectively. The results of FRAP assays suggest that the proteins in cytoplasmic speckles lack mobility and structural integrity, on the contrary, the proteins inside the aggresome can be functional and reversibly diffuse into the cytoplasm. As a result of these observations, aggresome formation via LLPS may function as a cytoprotective PQC by serving as a reversible temporary storage site for excessive amounts of proteins.

Meanwhile, recent studies have revealed that liquid droplets formed through LLPS are selectively degraded by autophagy [42-45]. In the case of selective autophagic degradation of stress granules, APE1 complex, and p62 bodies generated through LLPS, the liquidity of the condensates as well as the interacting proteins have been shown to be critical factors for the selective autophagy [44, 46]. Accumulating evidence indicates that proteins deposited in the aggresome can be cleared by autophagy [25, 47]. The aggresome as a gel-like state confirmed through data not only provides a way for rapid recovery of proteins through spatiotemporal sequestration but also suggests that it can provide adequate liquidity for subsequent degradation by selective autophagy.

The underlying mechanism for the dynamic of aggresome is still unsolved, and further evidence is still needed. It is unclear which protein leads the LLPS to form aggresome, why it has a gel-like structure rather than a typical liquid droplet generated through LLPS, and what factors induce the phase transition or maintain the phase in the aggresome. In this study, I showed the dynamic exchange of p62 or ubiquitin between the aggresome and surrounding environment by FRAP assay. This result raises the possibility of p62 and ubiquitin as candidates contributing to the dynamic characteristics of the aggresome. Notably, recent evidence suggests that p62 forms spherical liquid-like condensates. p62 contains an N-terminal PB1 domain, which drives its oligomerization, and a C-terminal UBA domain for its interaction with ubiquitin [48]. The critical role of p62 appears to be dependent on these two domains. Polymerization of p62 and the interaction between ubiquitin chains and p62 through these domains play critical roles in p62 phase separation which confer liquid-like properties [49, 50]. The valence of polyubiquitin can also affect p62 phase separation and transitions [50, 51]. Moreover, in terms of aggresome formation, p62 binds to polyubiquitinated proteins followed by its

oligomerization depending on these domains and directs them to the aggresome. These data collectively suggest that p62 and polyUb play an important role in determining the dynamic properties of the aggresome along with the formation of aggresomes. Although the precise molecular requirements for LLPS transitions in the aggresome need further investigation, this study allows us a better understanding of the aggresome as a gel-like condensate.

References

1. Shin, Y. and C.P. Brangwynne, *Liquid phase condensation in cell physiology and disease.* Science, 2017. **357**(6357).
2. Pappu, R.V., *Phase Separation-A Physical Mechanism for Organizing Information and Biochemical Reactions.* Dev Cell, 2020. **55**(1): p. 1-3.
3. Wang, B., et al., *Liquid-liquid phase separation in human health and diseases.* Signal Transduct Target Ther, 2021. **6**(1): p. 290.
4. Banani, S.F., et al., *Biomolecular condensates: organizers of cellular biochemistry.* Nat Rev Mol Cell Biol, 2017. **18**(5): p. 285-298.
5. Mitrea, D.M. and R.W. Kriwacki, *Phase separation in biology; functional organization of a higher order.* Cell Commun Signal, 2016. **14**: p. 1.
6. Molliex, A., et al., *Phase separation by low complexity domains promotes stress granule assembly and drives pathological fibrillization.* Cell, 2015. **163**(1): p. 123-33.
7. Aguzzi, A. and M. Altmeyer, *Phase Separation: Linking Cellular Compartmentalization to Disease.* Trends Cell Biol, 2016. **26**(7): p. 547-558.
8. Lin, Y., et al., *Formation and Maturation of Phase-Separated Liquid Droplets by RNA-Binding Proteins.* Mol Cell, 2015. **60**(2): p. 208-19.
9. Boeynaems, S., et al., *Protein Phase Separation: A New Phase in Cell Biology.* Trends Cell Biol, 2018. **28**(6): p. 420-435.
10. Patel, A., et al., *A Liquid-to-Solid Phase Transition of the ALS Protein FUS Accelerated by Disease Mutation.* Cell, 2015. **162**(5): p. 1066-77.
11. Snead, W.T. and A.S. Gladfelter, *The Control Centers of Biomolecular Phase Separation: How Membrane Surfaces, PTMs, and Active Processes Regulate*

Condensation. Mol Cell, 2019. **76**(2): p. 295-305.

12. Mann, J.R., et al., *RNA Binding Antagonizes Neurotoxic Phase Transitions of TDP-43.* Neuron, 2019. **102**(2): p. 321-338 e8.
13. Kostylev, M.A., et al., *Liquid and Hydrogel Phases of PrP(C) Linked to Conformation Shifts and Triggered by Alzheimer's Amyloid-beta Oligomers.* Mol Cell, 2018. **72**(3): p. 426-443 e12.
14. Chen, B., et al., *Cellular strategies of protein quality control.* Cold Spring Harb Perspect Biol, 2011. **3**(8): p. a004374.
15. Wickner, S., M.R. Maurizi, and S. Gottesman, *Posttranslational quality control: folding, refolding, and degrading proteins.* Science, 1999. **286**(5446): p. 1888-93.
16. Tyedmers, J., A. Mogk, and B. Bukau, *Cellular strategies for controlling protein aggregation.* Nat Rev Mol Cell Biol, 2010. **11**(11): p. 777-88.
17. Hartl, F.U., A. Bracher, and M. Hayer-Hartl, *Molecular chaperones in protein folding and proteostasis.* Nature, 2011. **475**(7356): p. 324-32.
18. Fredrickson, E.K. and R.G. Gardner, *Selective destruction of abnormal proteins by ubiquitin-mediated protein quality control degradation.* Semin Cell Dev Biol, 2012. **23**(5): p. 530-7.
19. Stolz, A. and D.H. Wolf, *Endoplasmic reticulum associated protein degradation: a chaperone assisted journey to hell.* Biochim Biophys Acta, 2010. **1803**(6): p. 694-705.
20. Johnston, J.A., C.L. Ward, and R.R. Kopito, *Aggresomes: a cellular response to misfolded proteins.* J Cell Biol, 1998. **143**(7): p. 1883-98.
21. Dikic, I., *Proteasomal and Autophagic Degradation Systems.* Annu Rev Biochem, 2017. **86**: p. 193-224.
22. Galluzzi, L., et al., *Molecular definitions of autophagy and related processes.*

EMBO J, 2017. **36**(13): p. 1811-1836.

23. Johnston, J.A., M.E. Illing, and R.R. Kopito, *Cytoplasmic dynein/dynactin mediates the assembly of aggresomes.* Cell Motil Cytoskeleton, 2002. **53**(1): p. 26-38.

24. Vallee, R.B. and P. Hook, *Autoinhibitory and other autoregulatory elements within the dynein motor domain.* J Struct Biol, 2006. **156**(1): p. 175-81.

25. Iwata, A., et al., *Increased susceptibility of cytoplasmic over nuclear polyglutamine aggregates to autophagic degradation.* Proc Natl Acad Sci U S A, 2005. **102**(37): p. 13135-40.

26. Waelter, S., et al., *Accumulation of mutant huntingtin fragments in aggresome-like inclusion bodies as a result of insufficient protein degradation.* Mol Biol Cell, 2001. **12**(5): p. 1393-407.

27. Ardley, H.C., et al., *Inhibition of proteasomal activity causes inclusion formation in neuronal and non-neuronal cells overexpressing Parkin.* Mol Biol Cell, 2003. **14**(11): p. 4541-56.

28. Okatsu, K., et al., *p62/SQSTM1 cooperates with Parkin for perinuclear clustering of depolarized mitochondria.* Genes Cells, 2010. **15**(8): p. 887-900.

29. Behl, C., *BAG3 and friends: co-chaperones in selective autophagy during aging and disease.* Autophagy, 2011. **7**(7): p. 795-8.

30. Watanabe, Y. and M. Tanaka, *p62/SQSTM1 in autophagic clearance of a non-ubiquitylated substrate.* J Cell Sci, 2011. **124**(Pt 16): p. 2692-701.

31. Choi, W.H., et al., *Aggresomal sequestration and STUB1-mediated ubiquitylation during mammalian proteaphagy of inhibited proteasomes.* Proc Natl Acad Sci U S A, 2020. **117**(32): p. 19190-19200.

32. Takayama, K., A. Matsuura, and E. Itakura, *Dissection of ubiquitinated protein*

degradation by basal autophagy. FEBS Lett, 2017. **591**(9): p. 1199-1211.

33. Nakajima, Y. and S. Suzuki, *Environmental stresses induce misfolded protein aggregation in plant cells in a microtubule-dependent manner.* Int J Mol Sci, 2013. **14**(4): p. 7771-83.

34. Alshareedah, I., T. Kaur, and P.R. Banerjee, *Methods for characterizing the material properties of biomolecular condensates.* Methods Enzymol, 2021. **646**: p. 143-183.

35. Riemenschneider, H., et al., *Gel-like inclusions of C-terminal fragments of TDP-43 sequester stalled proteasomes in neurons.* EMBO Rep, 2022. **23**(6): p. e53890.

36. Corboy, M.J., P.J. Thomas, and W.C. Wigley, *Aggresome formation.* Methods Mol Biol, 2005. **301**: p. 305-27.

37. Garcia-Mata, R., Y.S. Gao, and E. Sztul, *Hassles with taking out the garbage: aggravating aggresomes.* Traffic, 2002. **3**(6): p. 388-96.

38. Garcia-Mata, R., et al., *Characterization and dynamics of aggresome formation by a cytosolic GFP-chimera.* J Cell Biol, 1999. **146**(6): p. 1239-54.

39. Duster, R., et al., *1,6-Hexanediol, commonly used to dissolve liquid-liquid phase separated condensates, directly impairs kinase and phosphatase activities.* J Biol Chem, 2021. **296**: p. 100260.

40. Itoh, Y., et al., *1,6-hexanediol rapidly immobilizes and condenses chromatin in living human cells.* Life Sci Alliance, 2021. **4**(4).

41. Kaganovich, D., R. Kopito, and J. Frydman, *Misfolded proteins partition between two distinct quality control compartments.* Nature, 2008. **454**(7208): p. 1088-95.

42. Yamasaki, A., et al., *Liquidity Is a Critical Determinant for Selective Autophagy of Protein Condensates.* Mol Cell, 2020. **77**(6): p. 1163-1175 e9.

43. Buchan, J.R., et al., *Eukaryotic stress granules are cleared by autophagy and*

Cdc48/VCP function. Cell, 2013. **153**(7): p. 1461-74.

44. Zhang, G., et al., *mTOR Regulates Phase Separation of PGL Granules to Modulate Their Autophagic Degradation.* Cell, 2018. **174**(6): p. 1492-1506 e22.

45. Zaffagnini, G., et al., *p62 filaments capture and present ubiquitinated cargos for autophagy.* EMBO J, 2018. **37**(5).

46. Kageyama, S., et al., *p62/SQSTM1-droplet serves as a platform for autophagosome formation and anti-oxidative stress response.* Nat Commun, 2021. **12**(1): p. 16.

47. Olzmann, J.A., L. Li, and L.S. Chin, *Aggresome formation and neurodegenerative diseases: therapeutic implications.* Curr Med Chem, 2008. **15**(1): p. 47-60.

48. Berkamp, S., S. Mostafavi, and C. Sachse, *Structure and function of p62/SQSTM1 in the emerging framework of phase separation.* FEBS J, 2021. **288**(24): p. 6927-6941.

49. Fu, A., et al., *p62-containing, proteolytically active nuclear condensates, increase the efficiency of the ubiquitin-proteasome system.* Proc Natl Acad Sci U S A, 2021. **118**(33).

50. Sun, D., et al., *Polyubiquitin chain-induced p62 phase separation drives autophagic cargo segregation.* Cell Res, 2018. **28**(4): p. 405-415.

51. Dao, T.P. and C.A. Castaneda, *Ubiquitin-Modulated Phase Separation of Shuttle Proteins: Does Condensate Formation Promote Protein Degradation?* Bioessays, 2020. **42**(11): p. e2000036.

국문초록

액체-액체 상 분리를 통해 형성된 젤과 같은 구조를 갖는 응집소체

서울대학교 대학원

의과학과 의과학전공

박 서 형

액체-액체 상 분리 (LLPS)는 자유 에너지를 최소화하는 열역학적 과정으로, 혼합물을 두 개의 상으로 분리하여 세포 내에서 막 없는 소기관 (membrane-less organelles)의 형성을 가능하게 한다. 다양한 세포 내 스트레스는 P 바디 (P-body), 스트레스 과립 (stress granules)과 같이 막 없이 주변과 분리된 생분자응집체의 형성을 유도한다. 프로테아좀 (proteasome) 활성이 저해되면 유비퀴틴 접합체와 다양한 단백질들은 핵 주위 응집소체 (aggresome)로 격리되며, 응집소체는 단백질 품질 관리를 위한 선별 지점으로 기능한다. 본 논문에서는 응집소체가 상분리를 통해 형성되며, 액체와 고체 사이의 젤과 같은 특성을 보임을 밝혔다. 형광 광표백 (FRAP) 기법을 수행하였을 때, 다른

잘 알려진 액체 방울 (liquid droplet)에 비하여 응집소체의 형광 회복 속도가 감소해 있음을 확인하였으며, 액체 방울을 용해하는 1,6-헥산디올의 처리는 응집소체를 빠르게 용해하지 못하는 것을 관찰하였다. 또한, 응집소체의 형성 과정을 억제하는 것은 독성이 있는 불용성의 세포질 반점 (cytoplasmic speckle)을 초래함을 확인하였다. 따라서 본 논문에서는 응집소체를 젤과 같은 특성을 지닌 세포 내 막 없는 소기관 모델로 제시하였으며, 이들의 가역적인 응집은 세포 보호적 특성을 지니며 아밀로이드 생성 단백질 (amyloidogenic proteins)의 불용성 응집체 형성에도 관여할 것을 암시한다.

* 본 논문의 내용은 출판을 위해 더 연구 중에 있다.

주요어 : 프로테아좀, 응집소체, 막 없는 소기관, 액체-액체 상 분리

학 번 : 2020-22378